*Astronomy & Astrophysics* manuscript no. astroph
April 1, 2008




Letter to the Editor

# First detection of CO in a high-redshift damped Lyman-$\alpha$ system$^\star$

R. Srianand[1], P. Noterdaeme[2,3], C. Ledoux[2], and P. Petitjean[3]

[1] IUCAA, Post Bag 4, Ganeshkhind, Pune 411 007, India
[2] European Southern Observatory, Alonso de Córdova 3107, Casilla 19001, Vitacura, Santiago 19, Chile
[3] UPMC Paris 06, Institut d'Astrophysique de Paris, UMR7095 CNRS, 98bis Boulevard Arago, F-75014, Paris, France

Received date / Accepted date

**ABSTRACT**

We present the first detection of carbon monoxide (CO) in a damped Lyman-$\alpha$ system (DLA) at $z_{\rm abs}$ =2.41837 toward SDSS J143912.04+111740.5. We also detected $H_2$ and HD molecules. The measured total column densities (in log units) of H I, $H_2$, and CO are 20.10±0.10, 19.38±0.10, and 13.89±0.02, respectively. The molecular fraction, $f = 2N(H_2)/(N(H\,I)+2N(H_2)) = 0.27^{+0.10}_{-0.08}$, is the highest among all known DLAs. The abundances relative to solar of S, Zn, Si, and Fe are −0.03±0.12, +0.16±0.11, −0.86±0.11, and −1.32±0.11, respectively, indicating a high metal enrichment and a depletion pattern onto dust-grains similar to the cold ISM of our Galaxy. The measured $N(CO)/N(H_2) = 3\times10^{-6}$ is much less than the conventional $CO/H_2$ ratio used to convert the CO emission into gaseous mass but is consistent with what is measured along translucent sightlines in the Galaxy. The CO rotational excitation temperatures are higher than those measured in our Galactic ISM for similar kinetic temperature and density. Using the C I fine structure absorption lines, we show that this is a consequence of the excitation being dominated by radiative pumping by the cosmic microwave background radiation (CMBR). From the CO excitation temperatures, we derive $T_{\rm CMBR}$ = 9.15±0.72 K, while 9.315±0.007 K is expected from the hot big-bang theory. This is the most precise high-redshift measurement of $T_{\rm CMBR}$ and the first confirmation of the theory using molecular transitions at high redshift.

**Key words.** Galaxies: abundances – Quasars: absorption lines – Quasars: individual: SDSS J143912.04+111740.5

## 1. Introduction

Damped Lyman-$\alpha$ systems (DLAs) in QSO spectra are characterized by very high H I column densities, $N(H\,I)\gtrsim 10^{20}$ cm$^{-2}$. The inferred metallicities relative to solar vary between [Zn/H]= −2.0 and 0 for $2 \le z_{\rm abs} \le 3$ (e.g. Pettini et al. 1997; Prochaska & Wolfe 2002). Therefore DLAs are believed to be located in the close vicinity of star-forming regions. The dust content in a typical DLA is less than or equal to 10% of what is seen in the Galactic ISM for similar $N$(H I), however sufficient for favoring the formation of $H_2$ (Ledoux et al. 2003).

The abundance of $H_2$, the relative populations of the $H_2$ rotational levels, and the fine-structure levels of the C I ground-state are used to derive the physical conditions in the gas, such as temperature, gas pressure, and ambient radiation field (Savage et al. 1977; Black & van Dishoeck 1987; Jenkins & Tripp 2000; Tumlinson et al. 2002). These conditions are believed to be driven by the injection of energy and momentum through various dynamical and radiative processes associated with star formation activity. Thus, detecting $H_2$ in DLAs at high redshifts is an important step forward in understanding the evolution of normal galaxies. Detecting other molecules would pioneer interstellar chemistry studies at high redshift (see e.g. Wiklind & Combes 1995 for the dense ISM component).

In the course of our recently completed Very Large Telescope survey for $H_2$ in DLAs, we gathered a sample of 13 $H_2$ absorption systems at $1.8 < z < 4.3$ out of a total of 77 DLAs (Ledoux et al. 2003 & 2006; Petitjean et al. 2006; Noterdaeme et al. 2008). Absorption lines of HD are detected in one of the DLAs (Varshalovich et al. 2001) and none show detectable CO absorption. We noticed a strong preference for $H_2$-bearing DLAs being associated with C I absorption (Srianand et al. 2005) and having high metallicities and large depletion factors (Petitjean et al. 2006; Noterdaeme et al. 2008). In the Sloan Digital Sky Survey data base, we identified a most promising candidate at $z_{\rm abs}$ = 2.4185 towards SDSS J143912.04+111740.5 showing such characteristics. We were allocated 8 hours of director discretionary time on the Ultraviolet and Visual Echelle Spectrograph (UVES) at the VLT of the European Southern Observatory (ESO) to search for CO in addition to $H_2$. This observation resulted in the detection of CO UV absorption lines that have been elusive for more than a quarter century (Varshalovich & Levshakov 1981; Srianand & Petitjean 1998; Cui et al. 2005). We also detect $H_2$ and HD absorption lines. In this letter we focus our attention on the CO excitation. A detailed analysis of the HD absorptions will be presented elsewhere.

*Send offprint requests to*: R. Srianand, anand@iucaa.ernet.in

$^\star$ Based on observations carried out at the European Southern Observatory (ESO), under programme 278.A-5062 with the UVES echelle spectrograph installed at the ESO Very Large Telescope (VLT), unit Kueyen, on Mount Paranal in Chile.

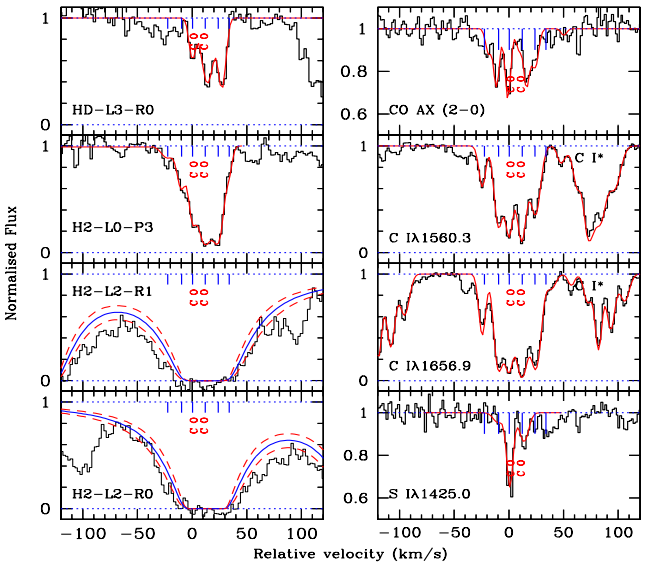


**Fig. 1.** A sample of molecular and heavy element absorption lines associated with the damped Lyman-$\alpha$ system toward SDSS J143912.04+111740.5. The normalized flux is given on a velocity scale with the origin at $z_{\rm abs} = 2.41837$. Smooth curves in each panel show our Voigt profile fits to the data. The dashed profiles shown for J$\leq$ 1 $H_2$ lines are the $1\sigma$ ranges. Tick marks in each panel indicate the locations of the 6 components that are used to fit the J = 3 $H_2$ absorption lines. The symbol "CO" marks the locations of two components detected in S I and CO.

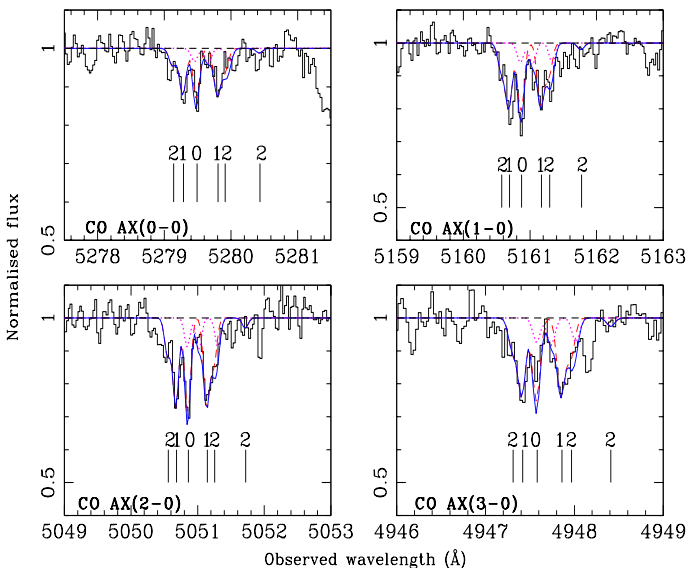


**Fig. 2.** Voigt profile fits to $^{12}$CO A-X bands detected at $z_{\rm abs} = 2.4185$ towards SDSS J143912.04+111740.5. The vertical lines mark the locations of CO absorptions from different J levels at the redshift of the main component. The profiles in dashed and dotted lines are, respectively, for the first and second components (at $z_{\rm abs} = 2.41837$ and 2.41847) and the total profile is shown in solid line.

## 2. Observations

Both UVES spectrographic arms were used with standard dichroic settings and central wavelengths of 390 nm and 580 nm (or 610 nm) for the blue and red arms, respectively. The resulting wavelength coverage was 330−710 nm with a small gap between 452 and 478 nm. The CCD pixels were binned $2 \times 2$ and the slit width adjusted to $1''$, yielding a resolving power of $R = 45000$ under seeing conditions of $\sim 0''.9$. The total exposure time on source exceeded 8 h. The data were reduced using the UVES pipeline version 3.3.1 based on the ESO common pipeline library system (Møller Larsen et al. 2007). Wavelengths were rebinned to the heliocentric rest frame and individual scientific exposures co-added. In the following, we adopt the solar reference abundances from Morton (2003).

## 3. Analysis

An asymmetric Lyman-$\alpha$ absorption line, together with the corresponding Lyman-$\beta$ and $\gamma$ absorption lines, indicates the presence of multiple components. The simultaneous fit to the three H I absorption features gives log $N$(H I) (cm$^{-2}$) = 17.8, 19.25, 19.20, 19.40, and 20.10±0.10 at the velocities of $v$ = −892, −594, −382, −117, and 0 km s$^{-1}$ relative to $z_{\rm abs} = 2.41837$. The component with maximum H I column density (at $v$ = 0 km s$^{-1}$) also exhibits $H_2$, HD, and CO absorption lines spread over ∼50 km s$^{-1}$ (see Fig. 1). Transitions from the J = 3 $H_2$ rotational level are detected in six distinct components. Both HD and CO are detected in three and two of these components, respectively. Transitions from J = 0 and 1 $H_2$ rotational levels are highly saturated, but accurate integrated column densities can be derived from damped wings.

Absorption lines from N I, O I, C I, C I*, C I**, Mg I, Ar I, S I, S II, Si II, Fe II, Zn II, Al II, and Ni II are seen spread over up to 950 km s$^{-1}$. The total gaseous abundances relative to solar are −0.03±0.12, +0.16±0.11, −0.86±0.11, and −1.32±0.11 for S, Zn, Si, and Fe, respectively. The abundances of S and Zn are consistent with the gas abundance being close to solar, while the relative depletions of Si and Fe are similar to those in cold gas in the diffuse Galactic ISM. Absorption lines from the three C I ground-state fine-structure levels are detected in numerous transitions in the main H I component.

In Fig. 1 we show a few transitions from $H_2$ (J = 0, 1 and 3), S I, C I, HD and CO. By fitting the damping wings of J = 0 and 1 transitions, we measured log $N$($H_2$, J=0) = 18.90±0.10 and log $N$($H_2$, J=1) = 19.18±0.10. We derived an excitation temperature of $T_{01} = 105^{+42}_{-32}$ K, which is usually a good indicator of the average kinetic temperature of the gas. The mean molecular fraction of the gas is $f = 2N(H_2)/[2N(H_2)+N(H\ I)] = 0.27^{+0.10}_{-0.08}$. This is the highest value measured to date in a high-$z$ DLA.

### 3.1. The CO molecules and the CO/$H_2$ ratio at high $z$

Carbon monoxide absorption was detected in several bands (see Fig. 2). We used the four bands that are redshifted outside the Lyman-$\alpha$ forest to derive CO column densities. Absorptions from different CO rotational levels are located close to each other, but the resolution of the data is high enough to deblend them. A single-component Voigt profile fit gives $z_{\rm abs} = 2.41837$ for the main CO component. This is coincident within error (<1 km s$^{-1}$) with the strongest S I component (See Fig. 2). A weaker S I satellite component is present at $z_{\rm abs} = 2.41853$. We therefore added a second CO

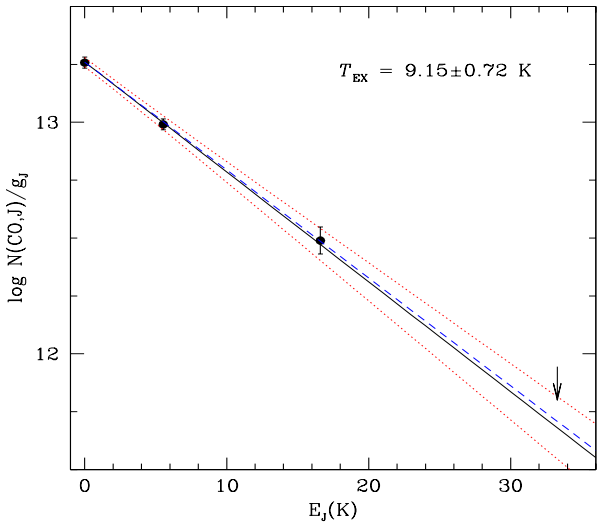


**Fig. 3.** The CO excitation diagram. A straight line with slope $1/(T_{\rm ex}$ ln 10) indicates thermalization of the levels. The diagram is given for the main CO component at $z_{\rm abs} = 2.41837$. The three lines give the mean and $1\sigma$ range obtained from $T_{01}$, $T_{02}$, and $T_{12}$. The diagram is compatible with thermalization by a black-body radiation of temperature 9.15±0.72 K when $T_{\rm CMBR} = 9.315\pm0.007$ K (long dashed line) is expected at $z_{\rm abs} = 2.4185$ from the hot big-bang theory.

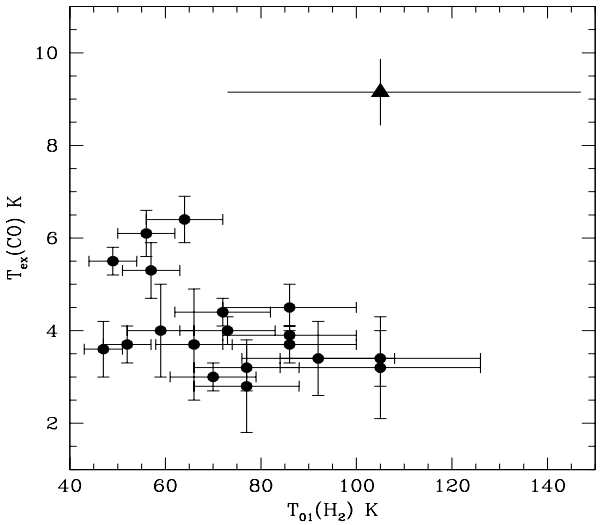


**Fig. 4.** Comparison of rotational excitation temperatures of CO and $H_2$ . Filled circles are for the measurements from Galactic diffuse ISM (Burgh et al. 2007). The filled triangle is for our measurement at $z = 2.4183$ towards SDSS J143912.04+111740.5.

component with a redshift fixed to the value of the second S I component. Doppler parameters were left free to vary and the best fit was obtained for $b = 1.5$ km s$^{-1}$, but the column density value in the main component is not very sensitive to the exact value for $b > 0.5$ km s$^{-1}$. Results are shown in Fig. 2. Column densities are log $N$(CO) = 13.27±0.03, 13.48±0.02, and 13.18±0.06, respectively, for J = 0, 1 and 2 in the main component. Column densities for J = 0 and 1 are 12.75±0.05 and 12.89±0.08 respectively for the second component when $b = 1.5$ km s$^{-1}$.

We measured $N({\rm CO})/N({\rm H_2}) = 3\times10^{-6}$. This is similar to or slightly higher than what is measured along the Galactic sightlines with similar molecular fraction and along Galactic sightlines with similar $N({\rm H_2})$ (see Figs. 4 and 5 of Burgh et al. 2007). This is much less than the CO/$H_2$ ratio of about $10^{-4}$ derived for dense molecular clouds (e.g Lacy et al. 1994). This strongly suggests that the physical conditions in the gas are similar to those in the diffuse Galactic ISM.

### 3.2. CO rotational excitation

The excitation temperatures derived from the population ratios of the different rotational levels are $T_{01} = 9.11 \pm 1.23$ K, $T_{12} = 9.19\pm1.21$ K, and $T_{02} = 9.16\pm0.77$ K for the main component where the errors come from the fitting uncertainties. Additional rms deviations come from uncertainties in the continuum placement and from the allowed range for the Doppler parameter of the second component. We estimate these to be ∼0.21, ∼0.37, and ∼0.18 K around the three excitation temperatures. The populations of the three rotational levels are thus consistent with a single excitation temperature, $T_{\rm ex} = 9.15 \pm 0.72$ K (see Fig. 3), suggesting that a single mechanism controls the level populations.

This excitation temperature is more than twice higher than the excitation temperature measured in the diffuse Galactic ISM (see Fig. 4), at similar $H_2$ $T_{01}$ (Burgh et al. 2007). Since we have seen that the physical conditions in the DLA are similar than in the diffuse Galactic ISM, we can suspect that the process responsible for this high excitation temperature is specific to the high redshift of the system. Interestingly, the population ratios in the second component are also consistent with this value of $T_{\rm ex}$, albeit with large errors.

The presence of absorptions from the three fine-structure levels of the C I ground state allows us to probe the physical state of the gas further (Srianand et al. 2000). By simultaneous Voigt profile fitting of the absorption lines, we derived log $N$(C I) = 14.26±0.01, log $N$(C I$^*$) = 14.02±0.02, and log $N$(C I$^{**}$) = 13.10±0.02 for the velocity component that corresponds to the strongest CO component. Assuming no contribution from the CMBR, we obtain a conservative hydrogen density range of 87-135 cm$^{-3}$ and 52-84 cm$^{-3}$ from the population ratios $N$(C I$^*$)/$N$(C I) and $N$(C I$^{**}$)/$N$(C I), respectively. A more realistic range, 45-62 cm$^{-3}$, is obtained if we use appropriate excitation by the CMBR with a temperature expected from the hot big-bang theory. From the observed $f$ value, we derived a conservative ($< 25$ cm$^{-3}$) and a realistic ($< 12$ cm$^{-3}$) value for the $H_2$ density ($n_{\rm H_2} = f n_{\rm HI}/(2-f)$). The above values are strict upper limits, because we have ignored the contribution of UV photons from stars in this galaxy to the C I excitation.

We ran the statistical equilibrium radiative transfer code RADEX, available on line (van der Tak et al. 2007), and found that for the kinetic temperature, $T = 105$ K, derived from $H_2$, the collisional contributions to $T_{01}$ and $T_{12}$ are ≤5% and ≤ 2% for $n_{\rm H_2} \leq 25$ cm$^{-3}$. The corresponding values are ≤ 3% and ≤1% for $n_{\rm H_2} \leq 12$ cm$^{-3}$. Thus the collisional excitation of CO by $H_2$ is negligible. Collisions with H contribute little to the CO excitation compared to collisions with $H_2$ in astrophysical conditions (Green &

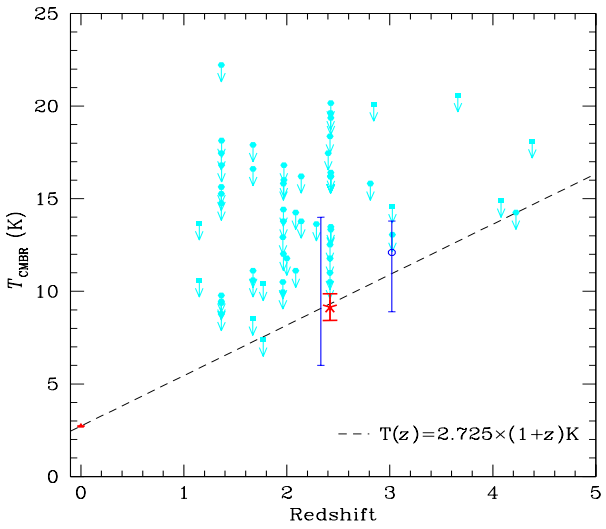


**Fig. 5.** Measurements of $T$(CMBR) at various $z$. The star with errorbars is for the measurement based on CO presented here. Our earlier measurement using fine-structure lines of neutral carbon, $6.0 < T_{\rm CMBR} < 14.0$ K, at z = 2.33771 is indicated by the long vertical bar (Srianand et al. 2000). Measurement by Molaro et al. (2002) is marked by an open circle. Upper limits are measurements using C I or C II* from the literature (squares) and using C I from our UVES sample (hexagons). The dashed line is the prediction from the hot big-bang theory, $T_{\rm CMBR}(z)$=$T_{\rm CMBR}(z = 0) \times (1 + z)$. $T_{\rm CMBR}$ measurement at $z = 0$ is based on the COBE determination (Mather et al. 1999).

Thaddeus, 1976; Shepler et al. 2007). This means that the CO excitation is dominated by CMBR, so we conclude that $T_{\rm ex} = T_{\rm CMBR} = 9.15\pm0.72$K.

## 4. Conclusion

The CMBR is an important source of excitation for those species with transitions in the sub-millimeter range. This is the case for atomic species whose ground state splits into several fine-structure levels and of molecules that can be excited in their rotational levels. If the relative level populations are thermalized by the CMBR, then the excitation temperature gives the temperature of the black-body radiation. It has long been proposed to measure the relative populations of such atomic levels in quasar absorption lines to derive $T_{\rm CMBR}$ at high redshift (Bahcall & Wolf 1968). In Fig. 5 we combine our precise measurement of $T_{\rm CMBR}$, the 51 new upper limits obtained using C I and C I* absorption lines detected towards QSOs in our UVES sample (Srianand et al. 2005; Noterdaeme et al. 2007a, 2007b; Ledoux et al. 2006), and measurements reported from the literature (Meyer et al. 1986; Songaila et al. 1994; Lu et al. 1996; Ge et al. 1997; Roth & Bauer, 1999; Molaro et al. 2002, Cui et al. 2005). Upper limits are obtained assuming CMBR as the only source of excitation. Our precise measurements using CO and the new upper limits using C I are consistent with the adiabatic evolution of $T_{\rm CMBR}$ expected in the standard big-bang model (Fig. 5).

The CN molecule has proven to be a remarkable thermometer of the CMBR in our Galaxy. It has been used for precise measurement of $T_{\rm CMBR}$ in different directions (Meyer et al. 1985; Kaiser et al. 1990). Wiklind & Combes (1996) obtained $T_{\rm CMBR} < 6$ K at $z = 0.885$ using the absorption lines of CS, $H^{13}CO^+$, and $N_2H^+$. Carbon monoxide in diffuse gas provides an interesting possibility for measurements at high redshift, as the rotational energies between different rotational levels are close to $T_{\rm CMBR}$ at $z \geq 1$.

Following careful selection of the target, based on intensive observations at ESO-VLT, we have made the first detection of carbon monoxyde molecules in the diffuse ISM at high redshift. The analysis presented here pioneers interstellar chemistry studies at high redshift and demonstrates that, together with the detection of other molecules such as HD or CH, it will be possible to tackle important cosmological issues.

*Acknowledgements.* We warmly thank the Director Discretionary Time allocation committee and the ESO Director General, Catherine Cesarsky, for allowing us to carry out these observations. RS and PPJ gratefully acknowledge support from the Indo-French Center for the Promotion of Advanced Research (Centre Franco-Indien pour la Promotion de la Recherche Avancée) under contract No. 3004-3. PN is supported by an ESO PhD studentship.

## References

Bahcall, J. N. & Wolf, R. A. 1968, ApJ, 152, 701.
Black, J. H., & van Dishoeck, E. F. 1988, ApJ, 331, 986
Burgh, E. B., France, K. & McCandliss, S. R. 2007, ApJ, 658, 446.
Cui, Jun, Bechtold, J., Ge, Jian, & Meyer, D. M. 2005, ApJ, 633, 649
Ge, J., Bechtold, J. & Black, J. H. 1997, ApJ, 474, 67
Ge, J., Bechtold, J. & Kulkarni, V. P., 2001, ApJ, 547, L1
Green, S. & Thaddeus, P. 1976, ApJ, 205, 766
Jenkins, E. B & Tripp, T. M. 2001, ApJS, 137, 297
Kaiser, M. E. & Wright, E. L. 1990, ApJ, 356, L1
Lacy, J. H., Knacke, R., Geballe, T. R., & Tokunaga, A. T. 1994, ApJ, 428, L69
Ledoux, C., Petitjean, P., Fynbo, J. P. U., Møller, P. & Srianand, R. 2006, A&A, 457, 71.
Ledoux, C., Petitjean, P. & Srianand, R. 2003, MNRAS, 346, 209
Lu., L., Sargent, W. L. W., Barlow, T. A., Churchill, C. W. & Vogt, S. S. 1996, ApJS, 107, 475
Mather, J. C. et al. 1999, ApJ, 512, 511 bibitem Meyer, D. M. & Jura, M. A. 1985, ApJ, 297, 119
Meyer, D. M., York, D. G., Black, J. H., Chaffee, F. H. & Foltz, C. B. 1986, ApJ, 308, L37
Molaro, P., Levshakov, S. A., Dessauges-Zavadsky, M. & O'dorico, S. 2002, A&A, 381, L64
Møller Larsen, J., Ballester, P., D'Odorico, V., et al. 2007, ESO Astrophysics Symposia, Springer-Verlag, in press
Morton, D. C. 2003, ApJS, 149, 205
Noterdaeme, P., Petitjean, P., Srianand, R., Ledoux, C., Le Petit, F., 2007a, A&A, 469, 425
Noterdaeme, P., et al., 2007b, A&A, 474, 393
Noterdaeme, P., Ledoux, C., Petitjean, P., Srianand, R., 2008, A&A in press, arXiv:0801.3682
Pettini, M., Smith, L. J., King, D. L., & Hunstead, R. W. 1997, ApJ, 486, 665
Petitjean, P., Ledoux, C., Noterdaeme, P. & Srianand, R., 2006, A&A, 456, L9
Petitjean, P., Ledoux, C., Srianand, R., 2000, A&A, 364, L26
Prochaska, J., Wolfe, A. M., 2002, ApJ, 566, 68
Quast, R. Baade, R. & Reimers, D. , 2002, A&A, 386, 796
Roth, K. C. & Bauer, J. M. 1999, ApJ, 515, 57
Savage, B. D., Bohlin, R. C., Drake, J. F. & Budich, W. 1977, ApJ, 216, 291
Shepler, B. C. et al. 2007, A&A, 475, L15
Songaila, A. et al. 1994, Nature, 371, 43
Srianand, R., & Petitjean, P. 1998, A&A, 335, 33
Srianand, R., Petitjean, P. & Ledoux, C. 2000, Nature, 408, 931
Srianand, R., Petitjean, P., Ledoux, C., Ferland, G. & Shaw, G., 2005, MNRAS, 362, 549

Tumlinson, J., Shull, J. M., Rachford, B. L., et al. 2002, ApJ, 566, 857
van der Tak, F. F. S., Black, J. H., Schöier, F. L., Jansen, D. J. & van Dishoeck, E. F., 2007, A&A, 468, 627
Varshalovich, D. A., Ivanchik, A. V., Petitjean, P., Srianand, R., Ledoux, C. 2001, AstL, 27, 683
Varshalovich, D. A., & Levshakov, S. A. 1981, Pisma Astron. Zh., 7, 204
Wiklind, T., & Combes, F. 1995, A&A, 299, 382
Wiklind, T., & Combes, F. 1996, Nature, 379, 139